J O U R N A L O F
Ceramic
Processing Research

The electrical insulation characteristics of a glass adhesive process for the silicon MEMS element of a pressure sensor

Gon-Jae Lee[a,b,*] and Duck-Kyun Choi[a]

[a]*Department of Materials Science and Engineering, Hanyang University, Seoul, Korea*
[b]*R&D Center, Mando corporation, Sungnam, Korea*

Recently, the electrical performance requirements of the sensor elements used in electric vehicles have been strengthened. Automotive pressure sensors are manufactured by bonding metal diaphragms and MEMS sensing elements. The withstand voltage of the pressure sensor is greatly affected by the electrical characteristics of the adhesive material between the metal diaphragm and the MEMS sensing element connected to the vehicle body. In this study, the withstand voltage of the sensor element was analyzed using glass paste as the bonding material for the glass paste process. As a result, it was found that this voltage was greatly influenced by the remaining glass paste porosity remaining following the glass paste process, and also by the area and thickness of the glass paste. Therefore, it was found that the thickness and area of the glass paste should be optimized and that the internal porosity should be minimized to obtain excellent withstand voltage characteristics in the sensing device.

Keywords: Insulation, Glass paste, Bonding, Process, MEMS.

Introduction

In a car, pressure sensors are the most frequently used sensors for monitoring engine intakes, air conditioner refrigerant pressure, injection pressure, and brake oil pressure [1]. With the recent advances in eco-friendly cars and car performances in general, pressure sensors are required to cover a wider range of pressures across diverse applications such as gauging fuel pressure in the engine while showing reliability even in diverse environments [2-4, 14-16].

Depending on the pressure range and the media which transfers the pressure, a variety of pressure-sensing devices and packages may be used. Recently, silicon MEMS (Micro Electro Mechanical System) devices have been used to cover a wide range of pressure [5-8].

Since the media which transfer pressures in sensors for air, gas, water, oil, and refrigerant are chemically reactive, sensing devices that use metal diaphragms are used for their reliability [5-8].

When metal diaphragms are used to make detection devices, a metal strain gauge thin-film resistor will be formed in the upper region of the diaphragm. The thin-film resistor of a metal strain gauge has a lower sensitivity and limits the output noise when compared to the silicon MEMS-type piezoresistor. Also, the

production cost for metal resistors is high because thin-film resistor deposition needs to be performed for every diaphragm using a customized semiconductor fabrication process. On the other hand, MEMS elements have the advantage of lower production cost because the sensors may be mass-produced using a single silicon wafer production process [9-13, 16]. However, to take advantage of the high sensitivity of metal diaphragms and low costs of MEMS elements, the two parts need to be bonded using glass paste. The joint is where metal diaphragms and MEMS element are connected, and the insulation between these two parts determine the insulation of the sensor module and the withstand voltage.

In this paper, to test the insulation characteristics of a high-reliability pressure sensor that uses a metal diaphragm and silicon MEMS element, glass paste was used in the bonding process between the two parts, and the bonding process condition and the insulation and voltage of the formation were measured.

Experimental

Fig. 1 shows how the MEMS element was added on top of the metal diaphragm and why the structure requires an insulating property. The MEMS element was produced using the semiconductor manufacturing process and MEMS Process. For the metal diaphragm, SUS630 (stainless steel) was used and glass paste was used to bind the silicon MEMS element.

To a prevent reduction in the performance and maintain the melting point of the glass paste under 500 °C, the glass powder primarily composed of PbO and a

*Corresponding author:
Tel : +82-2-6188-3343
Fax: +82-2-6188-3990
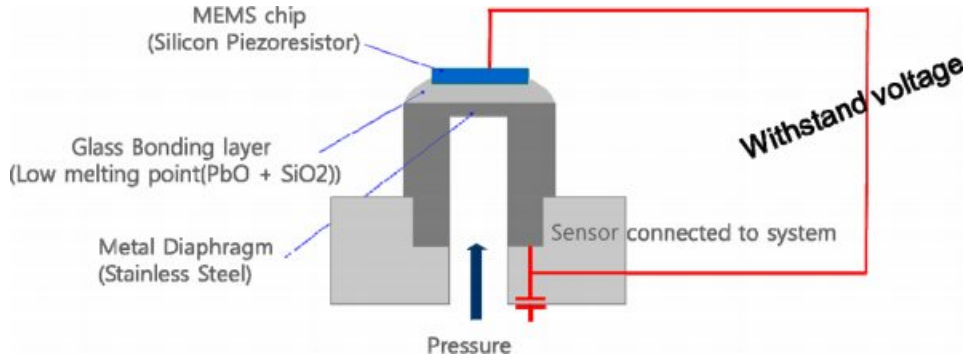E-mail: gonjae.lee@halla.com, gondolee@gmail.com

Fig. 1. A MEMS element bonding structure and electrical insulation structure on a metal diaphragm.

binding agent that helps to control the viscosity of the paste during printing process was also used.

To obtain the target viscosity, a ball mill was used for mixing, by increasing the rpm from 3 to 5 over a 60 min period. A screen printing process was used to apply glass paste on the metal diaphragm. When printing, the surface area and thickness were varied. The MEMS element was placed in the center of the glass paste, and for firing the glass paste, the temperature was increased at a rate of 6 °C/min until the temperature reached 420 °C and the temperature was then maintained for 10 minutes. To evaluate the withstand voltage of the sample processed using the glass paste, the silicon MEMS element was connected by wire bonding to a probe. Insulation resistance meters were used to measure the insulation voltage, which is reduced from the leakage current at 10 MWohm. The cross section of the bonding surface was analyzed to study the correlation between the insulation voltage and bonding structure. Further, to measure the withstand voltage of the sensor modules that use sensing elements, the withstand voltage was measured after the wire bonding of the sensing element and joints were potted with silicon gel in the protective process. The cross sections of the junctions were studied using an SEM (Scanning Electronic Microscope). To measure insulation voltage, an insulation voltage meter was used, and to measure the withstand voltage of the assembly of the sensor element, a withstand voltage meter was used.

Results and Discussion

Fig. 2 is a graph that plots viscosity as a function of the rolling speed and time, which are the process variables in the mixing process that are used to maintain a target viscosity before the glass paste undergoes the screen printing process. As shown in the graph, the viscosity is stabilized most quickly in the rolling speed range of 3-5 rpm. After a rolling time of 30 min, the viscosity was stabilized and no decrease in viscosity was observed.

After fixing the rolling speed at 5 rpm, the rolling time was increased from 0 to 60 min with a 10 min
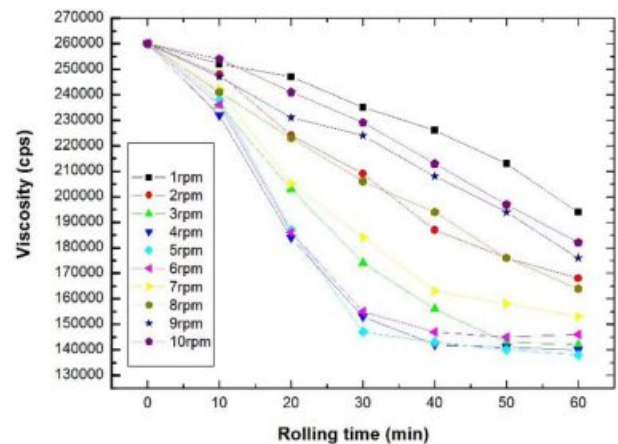

Fig. 2. The viscosity change according to the mixing process of the glass paste (rolling time and speed ball mill process).

increment. Using the screen printing process, glass pastes made with varying conditions were applied to the top of the metal diaphragm. After the silicon MEMS element was bonded on the applied glass paste, the glass paste underwent a firing process. Then, the insulation voltage was measured at the junction of the MEMS element of the sensing element and the metal diaphragm.

As shown in Fig. 3, the voltage saturates at 500 V when the rolling time reaches 30 min during the mixing process of the glass paste. This is also the point at which the viscosity is sufficiently stabilized.

To analyze the correlation between the glass paste thickness and insulation voltage, the glass paste thickness was controlled by controlling the mask thickness. To eliminate variables other than the thickness, the glass paste viscosity was fixed by fixing the rolling speed and time at 5 rpm and 40 min, respectively, as shown in Fig. 2, while the other process conditions were kept constant.

As shown in Fig. 4, which plots the insulation voltage as a function of the glass layer thickness, the insulation voltage was below 500 V when the thickness was less than 100 μm. At a thickness greater than 100 μm, the insulation voltage saturated at 500 V. This
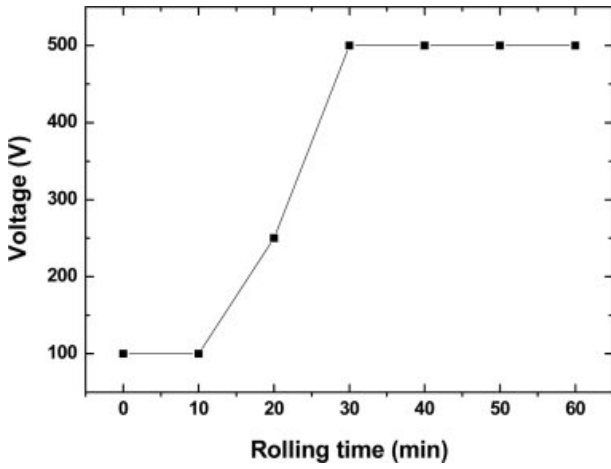
Fig. 3. The insulation voltage according to the rolling time during the mixing process of the glass paste.
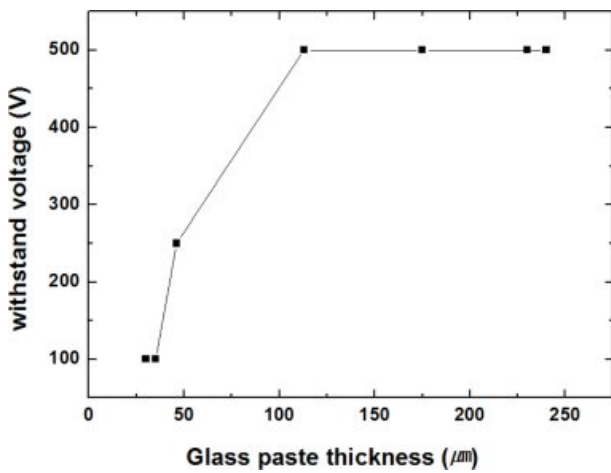

Fig. 4. The insulation performance with respect to glass layer thickness.

trend shows that increasing the glass layer thickness is positively correlated with the insulation voltage but

above a certain thickness, the insulation voltage saturates.

Fig. 5 shows the cross sections of the glass layers, which were processed at a rolling speed of 5 rpm, which is the point at which the viscosity is stabilized, as shown in Fig. 3, with multiple rolling times. As shown in the cross section, there are pores. The size of the pores and the porosity decreased as the rolling time increased from 0 to 40 minutes. Here, the porosity is defined as the ratio of the area of the pores per unit surface area of the glass layer in the observed picture: Porosity(%) = pore surface area/glass surface area (100 μm × 100 μm)*100%. The inverse relationship between the rolling time and porosity may be attributed to the fact that the glass powder and binder, which make up the glass paste, became homogeneous over time.

Fig. 6 is a schematic representation of the structure of Fig. 5. This schematic shows the difference in porosity inside the glass paste when the rolling process time is insufficient and sufficient.

Fig. 7 shows the correlation between the withstand voltage performance, which depends on the rolling time of the glass paste past from Fig. 3, and the porosity from Fig. 5. As rolling time increases up to 30 min, the porosity drops drastically and above 30 min, the porosity drops to about 0%. When the withstand voltage performance is viewed with respect to porosity, the withstand voltage increases as the porosity approaches 0%.

Additionally, when Fig. 5 was examined to identify the correlation between the porosity and thickness of the glass layer, which both affect the withstand voltage, for 3 different rolling times (0 min, 20 min, and 40 min) the thicknesses of the respective layers were 120 μm, 110 μm and 100 μm. Regardless of the thickness of the layer in Fig. 5, the porosity was high. High porosity has the effect of reducing the effective thickness and forming electrical paths, thereby lowering the withstand voltage. The correlation between the porosity and the thickness of the glass layer, which affects the

Rolling time	0 min	20 min	40 min
Cross section (by SEM)			
Pore size	2~4 μm	1~2 μm	No pore
Porosity	0.94 %	0.51 %	0.0075 %

Fig. 5. The cross-sectional observations (SEM) of glass pastes according to the rolling time (rolling speed: 5 rpm).
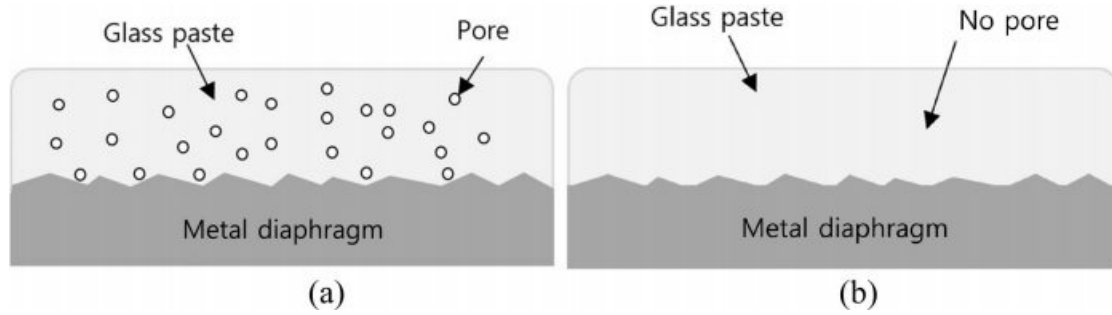
Fig. 6. Structural correlation of the glass paste between the rolling time and porosity a structure with insufficient rolling time and structure of the glass paste with sufficient rolling time.
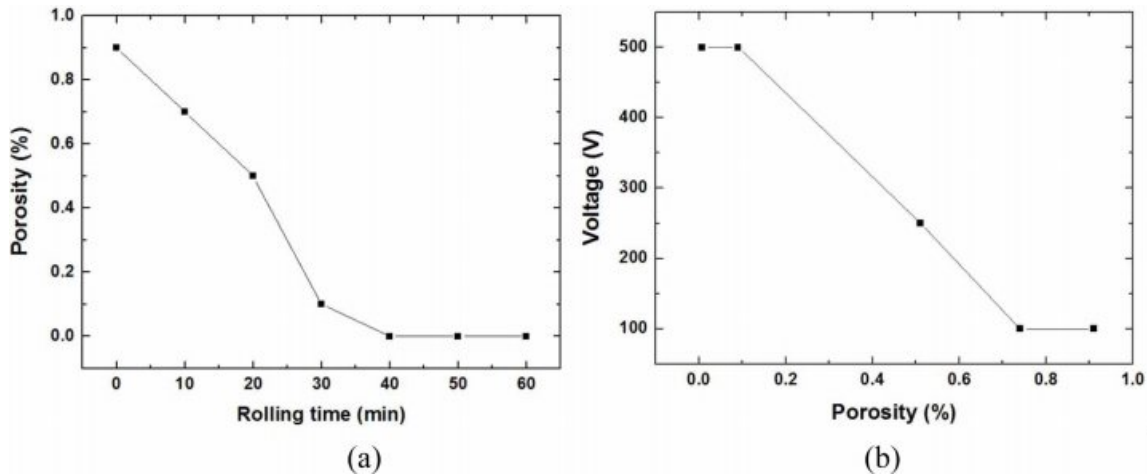

Fig. 7. The insulation performance with respect to porosity. (a) Porosity with respect to rolling time (rolling speed fixed at 5rpm) (b) insulation characteristics with respect to porosity..

withstand voltages in Figs. 4 and 5, is then explored. Regardless of the thickness, the higher the porosity, the lower the withstand voltage. It is considered that this is because when the porosity is high, the effective thickness is reduced and an electrical path of shorter distance is formed. Overall, it is concluded that the withstand voltage is determined by the thickness when the viscosity of the glass layer is stable.

Up to this point, the effect of the glass layer thickness on the withstand voltage was studied. Next, the study would like to shift the focus to the surface area on which glass paste is applied. To ensure good adhesion between the MEMS element and metal diaphragm, both the surface area and thickness, play an important role. Since the side length of the MEMS element and diaphragm may vary depending on the surface area, the effect of the surface area on the withstand voltage was analyzed.

From Fig. 8(a), we can see the top view of the MEMS element bonded on top of the glass paste printing on the diaphragm. To study the effect of the glass paste surface area, the size of the window for the metal mask used by the screen printing process was varied.

To distinguish the effect of the applied surface, we used the distance to the diaphragm when from the corner where the distance between the diaphragm and MEMS element was closest. When conducting this experiment, the viscosity of the glass paste was set to minimize the porosity by using a rolling speed of 5 rpm and a mixing time of 40 min.

The distance of the corner where glass paste was printed in between MEMS element and diaphragm was increased from 0.13~1.0 mm in 6 levels. Based on Fig. 8(b), which shows the insulation property as a function of the distance to the corner, the withstand voltage increases with the increase in the distance to the corner, until the distance reaches 0.3 mm, at which point interval voltage saturates at 500 V. In this observation, we can conclude that the withstand voltage performance is greater than or equal to 500 V above a 0.3 mm distance. We can see that to achieve the desired withstand voltage performance, there are correlations among the viscosity, thickness, and surface area of glass paste, which is used as the bonding agent between the Silicon MEMS element and metal diaphragm.
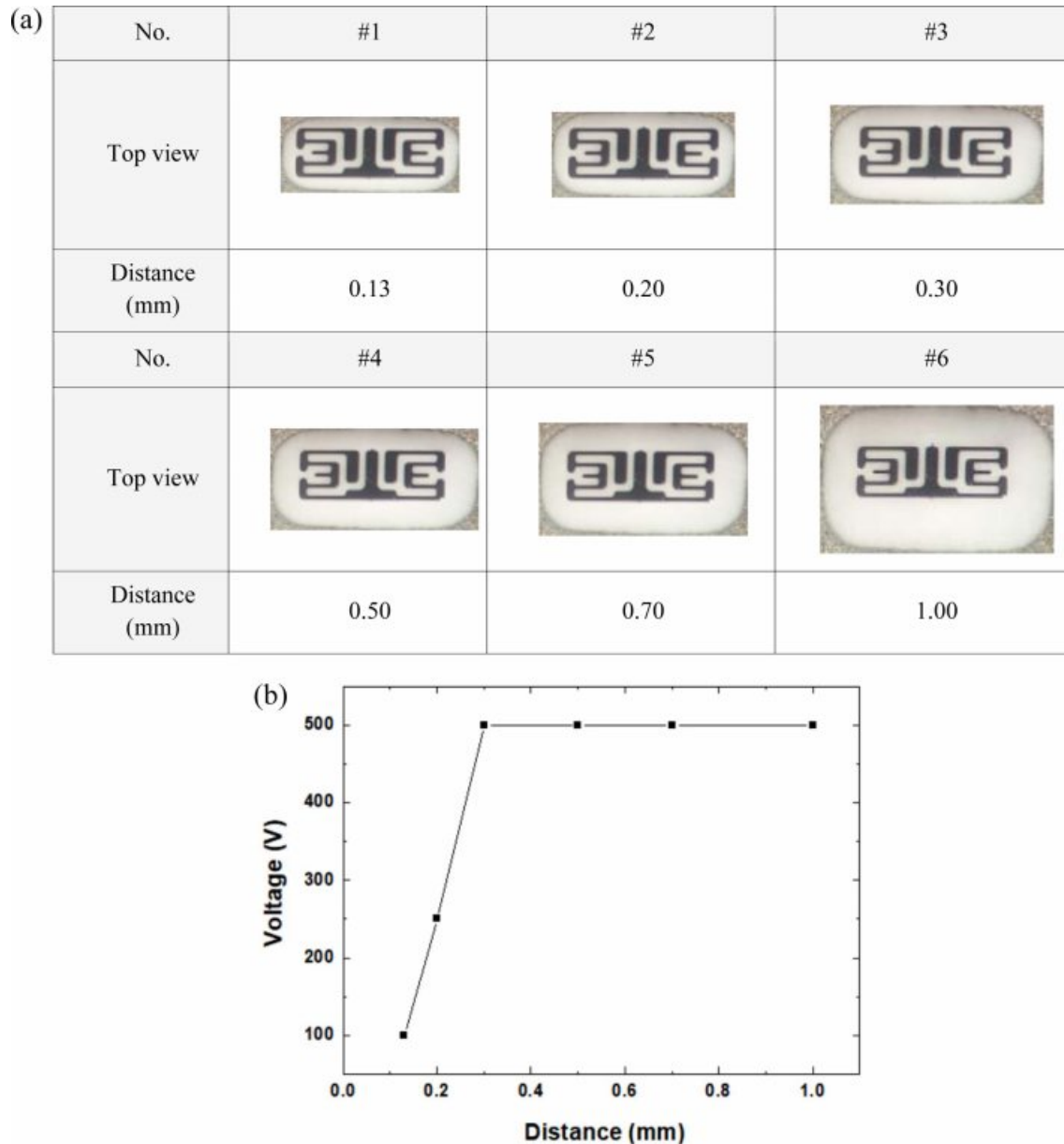
(a)

No.	#1	#2	#3
Top view			
Distance (mm)	0.13	0.20	0.30
No.	#4	#5	#6
Top view			
Distance (mm)	0.50	0.70	1.00

Fig. 8. (a) The top view of a Silicon MEMS element joined to the diaphragm surface along the surface on which the glass paste is applied. (b) The insulation voltage based on the length from the chip to the edge bonded from the glass paste.

Conclusions

The primary factors affecting the withstand voltage performance are the glass paste pore and thickness. Ball milling is the most important process for the pore control of the glass paste. With sufficient rolling time, the thickness of the glass bonding layer also must be more than a certain critical thickness of around 100 μm to satisfy the withstand voltage performance requirements. Additionally, it was found that a certain amount of surface area is required to achieve the desired withstand voltage when a MEMS element is bonded with glass paste. Therefore, it was found that the thickness and area of the glass bonding layer should be optimized and the withstand porosity should be minimized or removed to obtain excellent withstand voltage characteristics in the pressure sensor bonding of the MEMS element.

References

1. W.J. Fleming, Sens. J. IEEE 1[4] (2001) 296-308.
2. L. Boon-Brett, J. Bousek, and P. Moretto, Int. J. Hydrogen Energy. 34[1] (2009) 562-571.
3. L. Boon-Brett, J. Bousek, G. Black, P. Moretto, P. Castello, T. Hübert, and U. Banach, Int. J. Hydrogen Energy. 35[1] (2010) 373-384.
4. W. J. Buttner, M. B. Post, R. Burgess, and C. Rivkin, Int. J. Hydrogen Energy. 36[3] (2011) 2462-2470.
5. R. Singh, Low Lee Ngo, Ho Soon Seng, and F.N.C. Mok, in Proceeding of the First IEEE International Workshop on Electronic Design Test and Applications, January 2002,

edited by IEEE (IEEE, 2002) p. 181.

6. S.M. Sze, in "Semiconductor Sensors" (John Willey & Sons, 1994) p. 160-189.

7. K. N. Bhat and M. M. Nayak, J. ISSS. 2[1] (2013) 39-71.

8. L. Lin and W. Yun, in proceeding of Aerospace conference, March 1998, edited by IEEE (IEEE, 1998) p. 429-436.

9. D. S. Eddy and D. R. Sparks, in Proceeding of the IEEE, August 1998, edited by IEEE (IEEE, 1998) p. 1747.

10. S. Meti, K. B. Balavald, and B. G. Sheeparmatti, Int. J. Eng. Rese. Ind. Appl. 6[4] (2016) 23-31.

11. A. Hussain, M. Hannan, H. Sanusi, A. Mohamed, and B. Y. Majlis, J. Appl. Sci. 6[4] (2006) 810-815.

12. W. P. Eaton, J. H. Smith, D. J. Monk, G. O'Brien, and T. F. Miller, in Proceeding of SPIE, edited by SPIE (SPIE, 2007) p. 431-438.

13. M. Goel and S. Sharma, J. Electroceram. 12 (2004) 175-179.

14. H.-B. Jeon, I.-H. Lee, G. S. An, and Y.-S. Oha, J. Ceram. Process. Res. 19[6] (2018) 450-454.

15. K.-B. Kim, H.-K. Seok, Y.-S. Kim, J.-C. Yoon, D.-Y. Lee, C.-R. Chung, and D.-S. Han, J. Ceram. Process. Res. 7[3] (2006) 266-270.

16. G.-J. Lee and D.-K. Choi, J. Electroceram 41 (2018) 9-15.